Thin-film selective emitter

Donald L. Chubb
National Aeronautics and Space Administration, Lewis Research Center, Cleveland, Ohio 44135

Roland A. Lowe
Cleveland State University, Cleveland, Ohio 44115

(Received 19 April 1993; accepted for publication 12 July 1993)

Direct conversion of thermal energy into electrical energy using a photovoltaic cell is called thermophotovoltaic energy conversion. One way to make this an efficient process is to have the thermal energy source be an efficient selective emitter of radiation. The emission must be near the band-gap energy of the photovoltaic cell. One possible method to achieve an efficient selective emitter is the use of a thin film of rare-earth oxides. The determination of the efficiency of such an emitter requires analysis of the spectral emittance of the thin film including scattering and reflectance at the vacuum-film and film-substrate interfaces. Emitter efficiencies (power emitted in emission band/total emitted power) in the range 0.35–0.7 are predicted. There is an optimum optical depth to obtain maximum efficiency. High emitter efficiencies are attained only for low ($\leqslant 0.05$) substrate emittance values, both with and without scattering. The low substrate emittance required for high efficiency limits the choice of substrate materials to highly reflective metals or high-transmission materials such as sapphire.

I. INTRODUCTION

Thermophotovoltaic (TPV) energy conversion research dates back to the 1960s.[1,2] Most of the early studies[3–7] of TPV energy conversion used the solar flux as the thermal energy input. In those systems the solar energy was absorbed and reemitted, the idea being to improve the efficiency of the photovoltaic (PV) conversion by matching the spectrum of the radiation to the band gap of the PV cell. There is now renewed interest in TPV energy conversion for space power systems using nuclear energy sources[8,9] and also commercial combustion driven systems.[10]

The preferred emitter for the early solar driven systems[3–6] was a blackbody coupled with a bandpass filter. Ideally, only photons with energy greater than the PV cell band-gap energy are transmitted and all others are reflected back to the emitter to be reabsorbed. Thus, the emitter-filter combination performs as a selective emitter. For such systems to be efficient the filter absorptance must be low.[4,6] A simpler, efficient TPV system will be possible if an efficient selective emitter can be produced. In Ref. 7 a selective emitter is proposed for a solar TPV system.

The early work of White and Schwartz[11] recognized the benefits of selective emitters for efficient thermophotovoltaic energy conversion; however, finding an efficient selective emitter has been a difficult task. The most promising solid selective emitters have been the rare-earth elements.[12] For doubly and triply charged ions of these elements in crystals the orbits of the valence $4f$ electrons, which account for emission and absorption, lie inside the $5s$ and $5p$ electron orbits. As a result, the rare-earth ions in the solid state have radiative characteristics much like they would have if they were isolated. They emit in narrow bands rather than in a continuum as do most solids. The $5s$ and $5p$ electrons "shield" the $4f$ valence electrons from the surrounding ions in the crystal. The spectra of these rare-earth ions in crystals have been extensively studied. Most of this work is summarized in the text of Dieke.[13]

Early spectral emittance work[12] on rare-earth oxides that are suitable for TPV showed strong emission bands. However, the emittance for photon energies below the band gap for PV materials was also significant. As a result, the efficiency of these emitters was low. In the last few years, however, Nelson and Parent[14,15] have reported a large improvement in rare-earth oxide emitters. Their emitters are constructed of fine (5–10 μm) rare-earth oxide fibers similar to the construction of the Welsbach mantle used in gas lanterns. The very small characteristic dimension of these emitters results in a low emittance in the low-energy part of the spectrum, thus giving them a high efficiency. Chubb[16] has calculated the efficiency for the rare-earth emitters constructed with a small characteristic dimension and found that efficiencies approaching 80% are possible.

As already mentioned, major improvement in the rare-earth oxide emitters resulted from the small characteristic dimension possible with the mantle-type geometry. Another way to obtain a small characteristic dimension is to use a thin film. This geometry enables a smaller ($< 10\,\mu$m) characteristic dimension and thus higher efficiency. Also, a thin film on a strong substrate is more rugged than the mantle-type emitter.

To evaluate the potential of a thin-film selective emitter, the analysis described in this article was carried out. An expression for the spectral emittance of a thin film was derived using a continuum radiative transfer analysis that includes scattering. Using the derived spectral emittance, the emitter efficiency and power density were calculated. To model the photon energy dependence of the rare-earth oxide optical properties, the spectrum was split into three regions. Within each region the optical properties are assumed constant.

 0021-8979/93/74(9)/5687/12/$6.00

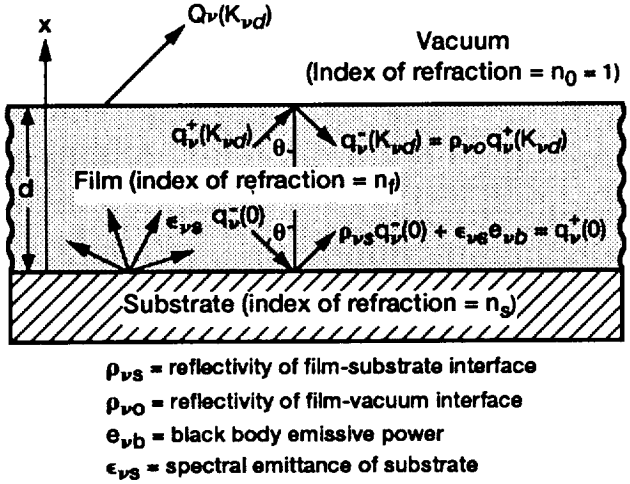

FIG. 1. Schematic of emitting film.

II. SPECTRAL EMITTANCE OF THIN FILM

In order to determine the efficiency of a thin-film selective emitter, the spectral emittance must be known. The following deriviation is based on the continuum radiation transfer equations.[17] Figure 1 shows the one-dimensional model of the film. The radiation intensity i_ν is assumed to vary only in the x direction. This is an excellent approximation for thin films where the film dimensions perpendicular to the x direction are much larger than the film thickness d. The radiative transfer equations for the spectral radiation intensities in the positive x direction i_ν^+ and the negative x direction i_ν^-, as functions of the optical depth K_ν and angle θ ($\mu=\cos\theta$) are the following:

$$i_\nu^+(K_\nu,\mu)=i_\nu^+(0,\mu)\exp\left(-\frac{K_\nu}{\mu}\right)+\int_0^{K_\nu} S_\nu(K_\nu^*,\mu)\times\exp\left(-\frac{K_\nu-K_\nu^*}{\mu}\right)\frac{dK_\nu^*}{\mu},\quad 0\leqslant\mu\leqslant 1, \tag{1}$$

$$i_\nu^-(K_\nu,\mu)=i_\nu^-(K_{\nu d},\mu)\exp\left(\frac{K_{\nu d}-K_\nu}{\mu}\right)-\int_{K_\nu}^{K_{\nu d}} S_\nu(K_\nu^*,\mu)\exp\left(\frac{K_\nu^*-K_\nu^*}{\mu}\right)\frac{dK_\nu^*}{\mu},\quad -1\leqslant\mu\leqslant 0. \tag{2}$$

And the source function S_ν for isotropic scattering satisfies the following equation:

$$S_\nu(K_\nu)=n_f^2(1-\Omega_\nu)i_{\nu b}+\frac{\Omega_\nu}{2}\left[\int_0^1 i_\nu^+(0,\mu)\exp\left(-\frac{K_\nu}{\mu}\right)d\mu+\int_0^1 i_\nu^-(K_{\nu d},-\mu)\exp\left(\frac{K_{\nu d}-K_\nu}{-\mu}\right)d\mu+\int_0^{K_{\nu d}} S_\nu(K_\nu^*)E_1(|K_\nu^*-K_\nu|)dK_\nu^*\right], \tag{3}$$

where n_f is the index of refraction of the film. Also, appearing in Eqs. (1)–(3) is the optical depth K_ν,

$$K_\nu(x)=\int_0^x(a_\nu+\sigma_\nu)dx^*=\int_0^x\alpha_\nu\,dx^*, \tag{4}$$

where a_ν is the spectral absorption coefficient, σ_ν is the scattering coefficient, and $\alpha_\nu=a_\nu+\sigma_\nu$ is the extinction coefficient. Also, the scattering albedo Ω_ν is defined as follows:

$$\Omega_\nu=\frac{\sigma_\nu}{a_\nu+\sigma_\nu}, \tag{5}$$

and the blackbody intensity $i_{\nu b}$ and hemispherical emissive power $e_{\nu b}$ are the following:

$$i_{\nu b}=\frac{e_{\nu b}}{\pi}=\frac{2h\nu^3}{c_0^2}\frac{1}{\exp(h\nu/kT)-1}, \tag{6}$$

where h is Planck's constant, k is Boltzmann's constant, and c_0 is the vacuum speed of light. Finally, the general exponential integral $E_n(u)$ is the following:

$$E_n(u)=\int_0^1 v^{n-2}\exp\left(-\frac{u}{v}\right)dv. \tag{7}$$

The following approximations were made to simplify the solution to Eqs. (1)–(3);

(1) The temperature T_E is uniform; therefore, a_ν, σ_ν, and n_f are constant throughout the film and $K_\nu=\alpha_\nu x$ and $K_{\nu d}=\alpha_\nu d$.

(2) The film is a pure dielectric; therefore n_f is a real number.

(3) Scattering is isotropic.

(4) Boundaries at $x=0$ and $x=d$ behave diffusively; therefore, $i_\nu^+(0)$, $i_\nu^-(K_{\nu d})$, and reflectivity at substrate-film interface $\rho_{\nu s}$, reflectivity at film-vacuum interface $\rho_{\nu 0}$, and emittance of substrate $\epsilon_{\nu s}$ are independent of θ.

(5) Interference effects are neglected although $d<\lambda$ for part of spectrum. Assuming diffuse boundaries yields the following boundary conditions at $x=0$ ($K_\nu=0$) and $x=d(K_\nu=K_{\nu d})$,

$$q_\nu^+(0)=\epsilon_{\nu s}e_{\nu b}+\rho_{\nu s}q_\nu^-(0),\quad K_\nu=0, \tag{8}$$

$$q_\nu^-(K_{\nu d})=\rho_{\nu 0}q^+(K_{\nu d}),\quad K_\nu=K_{\nu d}, \tag{9}$$

where

$$q_\nu^+(0)=2\pi\int_0^{\pi/2} i_\nu^+(0)\cos\theta\sin\theta\,d\theta=2\pi\int_0^1\mu i_\nu^+(0)d\mu=\pi i_\nu^+(0), \tag{10a}$$

and, similarly,

$$q_\nu^-(0)=\pi i_\nu^-(0), \tag{10b}$$

$$q_\nu^+(K_{\nu d})=\pi i_\nu^+(K_{\nu d}), \tag{10c}$$

$$q_\nu^-(K_{\nu d})=\pi i_\nu^-(K_{\nu d}). \tag{10d}$$

Since $i_\nu^+(0)$ and $i_\nu^-(K_{\nu d})$ are assumed independent of μ, the μ integration in Eq. (3) can be performed,

$$S_\nu(K_\nu)=n_f^2(1-\Omega_\nu)\frac{e_{\nu b}}{\pi}+\frac{\Omega_\nu}{2}\left[E_2(K_\nu)\frac{q_\nu^+(0)}{\pi}+E_2(K_{\nu d}-K_\nu)\frac{q_\nu^-(K_{\nu d})}{\pi}\right]+\int_0^{K_{\nu d}} S_\nu(K_\nu^*)E_1(|K_\nu^*-K_\nu|)dK_\nu^*. \quad (11)$$

This must be solved for $S_\nu(K_\nu)$ which can then be used in Eqs. (1) and (2). The method outlined in Ref. 8 was used to solve Eq. (11). Replacing the exponential integral functions in Eq. (11) with exponential approximations allows the integral equation to be converted to a linear second-order differential equation, which can be easily solved. Details of the solution are given in the Appendix.

The hemispherical spectral emittance is defined as follows:

$$\epsilon_\nu=\frac{Q_\nu(K_{\nu d})}{e_{\nu b}}, \quad (12)$$

where $Q_\nu(K_{\nu d})$ is the spectral emissive power at $K_\nu=K_{\nu d}$. To include the refractive properties of the film-vacuum interface the maximum angle θ_M that allows radiation to escape the film is given by Snell's law,

$$\mu_M^2\equiv\cos^2\theta_M=1-\left(\frac{1}{n_f}\right)^2. \quad (13)$$

For $\theta>\theta_M$ radiation is totally reflected. Including angles greater than θ_M would allow the possibility of $\epsilon_\nu>1$.[17] Therefore, using the boundary condition given by Eq. (9), the emissive power becomes

$$Q_\nu(K_{\nu d})=2\pi\int_0^{\theta_M}[i_\nu^+(K_{\nu d},\mu)-i_\nu^-(K_{\nu d},\mu)]\cos\theta\sin\theta\,d\theta=2\pi(1-\rho_{\nu 0})\int_0^1\mu i^+(K_{\nu d},\mu)d\mu. \quad (14)$$

Now, using Eq. (1) and the boundary condition given by Eq. (8) in Eq. (14),

$$Q_\nu(K_{\nu d})=(1-\rho_{\nu 0})\left[q_\nu^+(K_{\nu d})-2[\epsilon_{\nu s}e_{\nu b}+\rho_{\nu s}q^-(0)]\times\mu_M^2E_3\left(\frac{K_{\nu d}}{\mu}\right)-\Phi_M\right]. \quad (15)$$

The $q_\nu^+(K_{\nu d})$ and $q_\nu^-(0)$ terms are obtained from Eqs. (1) and (2) and the boundary conditions given by Eqs. (8) and (9),

$$q_\nu^+(K_{\nu d})=2\pi\int_0^1\mu i_\nu^+(K_{\nu d},\mu)d\mu=2[\epsilon_{\nu s}e_{\nu b}+\rho_{\nu s}q_\nu^-(0)]E_3(K_{\nu d})+\Phi_+ \quad (16)$$

$$q_\nu^-(0)=2\pi\int_0^1\mu i_\nu^-(0,\mu)d\mu=2\rho_{\nu 0}q_\nu^+(K_{\nu d})E_3(K_{\nu d})+\Phi_-. \quad (17)$$

The source term integrals appearing in Eqs. (15) to (17) are

$$\Phi_+=2\pi\int_0^{K_{\nu d}}S_\nu(K_\nu^*)E_2(K_{\nu d}-K_\nu^*)dK_\nu^*, \quad (18)$$

$$\Phi_M=2\pi\mu_M\int_0^{K_{\nu d}}S_\nu(K_\nu^*)E_2\left(\frac{K_{\nu d}-K_\nu^*}{\mu_M}\right)dK_\nu^*, \quad (19)$$

$$\Phi_-=2\pi\int_0^{K_{\nu d}}S_\nu(K_\nu^*)E_2(K_\nu^*)dK_\nu^*. \quad (20)$$

Using Eq. (A8) (see the Appendix) for S_ν in Eqs. (18)–(20) and the exponential approximation for E_2 [Eq. (A2)] results in the following after a great deal of algebra:

$$\Phi_M=l_1(\mu_M)q_\nu^+(0)+l_2(\mu_M)q_\nu^-(K_{\nu d})+l_3(\mu_M)e_{\nu b}, \quad (21)$$

$$\Phi_+=l_1(1)q_\nu^+(0)+l_2(1)q_\nu^-(K_{\nu d})+l_3(1)e_{\nu b}, \quad (22)$$

$$\Phi_-=l_2(1)q_\nu^+(0)+l_1(1)q_\nu^-(K_{\nu d})+l_3(1)e_{\nu b}, \quad (23)$$

where

$$l_1(\mu)=2\mu^2\gamma\left(\frac{a_2}{b_2}\right)\{A_4[m_2(\mu)A_2-m_1(\mu)A_1]-m_3(\mu)\}, \quad (24)$$

$$l_2(\mu)=2\mu^2\gamma\left(\frac{a_2}{b_2}\right)\{A_4[m_1(\mu)A_2-m_2(\mu)A_1]+m_0(\mu)\}, \quad (25)$$

$$l_3(\mu)=2n_f^2\mu^2\left\{\frac{1}{2}\left(\frac{1-\Omega_\nu}{1-z}\right)\left[1-2E_3\left(\frac{K_{\nu d}}{\mu}\right)\right]-A_3A_4[m_1(\mu)+m_2(\mu)]\frac{a_2}{b_2}\right\}, \quad (26)$$

$$m_1(\mu)=\frac{1}{1+\mu(\sqrt{1-z/u})}\left[1-\exp\left(-r-\frac{y}{\mu}\right)\right], \quad (27)$$

$$m_2(\mu)=\frac{1}{1+\mu(\sqrt{1-z/u})}(e^{-r}-e^{-y/\mu}), \quad (28)$$

$$m_3(\mu)=\frac{1}{1-\mu}(e^{-y}-e^{-y/\mu})\quad\text{for }\mu\neq 1, \quad (29)$$

$$m_3(1)=ye^{-y}, \quad (30)$$

$$m_0(\mu)=\frac{1}{1+\mu}\left[1-\exp\left(-\frac{y}{\mu}-y\right)\right], \quad (31)$$

$$A_1=\frac{w_+}{u+1}e^{-y}+\frac{w_-}{u-1}e^{-r}, \quad (32)$$

$$A_2=\frac{w_+}{u-1}+\frac{w_-}{u+1}\exp(-r-y), \quad (33)$$

$$A_3=\left(\frac{1-\Omega_\nu}{1-z}\right)(w_+-w_-e^{-r}), \quad (34)$$

$$A_4=\frac{z}{w_+^2-w_-^2e^{-2r}}, \quad (35)$$

$$w_+=1+\sqrt{1-z}, \quad (36)$$

$$w_- = 1 - \sqrt{1-z}, \tag{37}$$

$$\gamma = \frac{a_2 \Omega_\nu}{2\{1-[z/(1-u^2)]\}}, \tag{38}$$

$$r = b_1 \sqrt{1-z} K_{\nu d}, \tag{39}$$

$$y = b_2 K_{\nu d}, \tag{40}$$

$$z = \frac{a_1 \Omega_\nu}{b_1}, \tag{41}$$

$$u = \frac{b_2}{b_1}. \tag{42}$$

After using the boundary conditions [Eqs. (8) and (9)] in Eqs. (22) and (23) and substituting the results in Eqs. (16) and (17) we are left with two algebraic equations for $q_\nu^+(K_{\nu d})$ and $q_\nu^-(0)$. Solving these yields

$$q_\nu^+(K_{\nu d}) = \frac{e_{\nu b}}{\mathrm{DEN}} (\epsilon_{\nu s} L_1(1) + l_3(1) \times \{1 + \rho_{\nu s}[L_1(1) - l_2(1)]\}), \tag{43}$$

$$q_\nu^-(0) = \frac{e_{\nu b}}{\mathrm{DEN}} \{\epsilon_{\nu s}[L_2(1) l_2(1) + \rho_{\nu 0} L_1^2(1)] + l_3(1) \times [L_1(1) + L_2(1)]\}, \tag{44}$$

where

$$L_1(\mu) = l_1(\mu) + 2\mu^2 E_3\left(\frac{K_{\nu d}}{\mu}\right), \tag{45}$$

$$L_2(\mu) = 1 - \rho_{\nu 0} l_2(\mu), \tag{46}$$

$$\mathrm{DEN} = L_2(1)[1 - \rho_{\nu s} l_2(1)] - \rho_{\nu 0} \rho_{\nu s} L_1^2(1). \tag{47}$$

Using Eqs. (43), (44), and (21) in Eq. (15) the hemispherical spectral emittance is obtained,

$$\epsilon_\nu = \frac{Q_\nu(K_{\nu d})}{e_{\nu b}} = \frac{1-\rho_{\nu 0}}{\mathrm{DEN}} [\epsilon_{\nu s}[L_1(1) L_2(\mu_M) - L_1(\mu_M) L_2(1)] + l_3(1)(L_2(\mu_M) + \rho_{\nu s}\{[L_2(\mu_M) - \rho_{\nu 0} L_1(\mu_M)] \times [L_1(1) - l_2(1)] - L_1(\mu_M)\}) - l_3(\mu_M)\mathrm{DEN}]. \tag{48}$$

In Eq. (48) the contributions to ϵ_ν are split into two groups. The first group, which is proportional to $\epsilon_{\nu s}$, results from the substrate emittance. The second group, which is proportional to l_3, is the contribution of the film to the spectral emittance.

Consider two limiting solutions to Eq. (48). First, for $K_{\nu d} \to 0$ expand Eq. (48) in terms of $K_{\nu d}$ and retain only the linear $K_{\nu d}$ term. In this case the following is obtained:

$$\epsilon_{\nu 0} = \frac{(1-\rho_{\nu 0})(1-\mu_M)}{1-\rho_{\nu 0}\rho_{\nu s}} \left\{\epsilon_{\nu s}(1+\mu_M) + \left[2n_f^2\left(\frac{1-\Omega_\nu}{1-z}\right) \times (1-a_2 z)\{1+\rho_{\nu s}[1+\mu_M(1+\rho_{\nu 0})]\} - \epsilon_{\nu s}[2 - a_2^2 \Omega_\nu (1-\mu_M \rho_{\nu 0})]\right] K_{\nu d}\right\}. \tag{49}$$

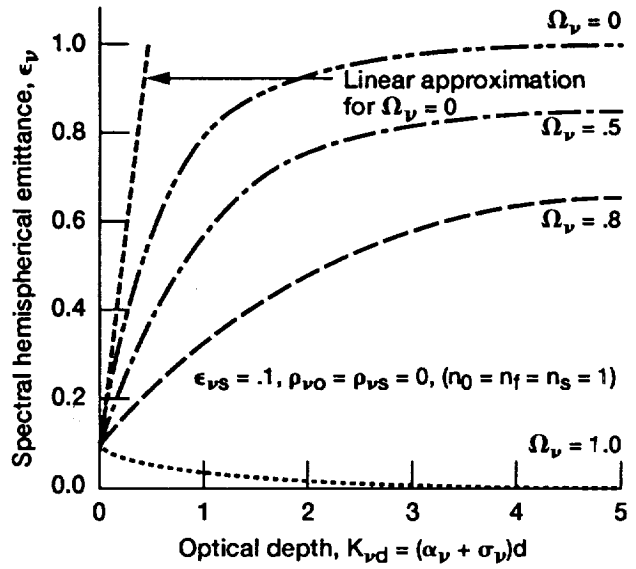

FIG. 2. Spectral hemispherical emittance ϵ_ν of emitting film for various values of scattering albedo Ω_ν, substrate emittance $\epsilon_{\nu s}=0.1$, and no reflection at interfaces ($\rho_{\nu 0}=\rho_{\nu s}=0$).

Second, for $K_{\nu d} \to \infty$ Eq. (48) becomes the following:

$$\epsilon_{\nu \infty} = \frac{1-\rho_{\nu 0}}{1-\rho_{\nu 0} l_2^\infty(1)} \{l_3^\infty(1) - l_3^\infty(\mu_M) - \rho_{\nu 0} \times [l_2^\infty(\mu_M) l_3^\infty(1) - l_2^\infty(1) l_3^\infty(\mu_M)]\}, \tag{50}$$

where

$$l_2^\infty(\mu) = 2\mu^2\left(\frac{\gamma}{1+\mu}\right)\left(\frac{a_2}{b_2}\right) \times \left[1 - \frac{z}{w_+(1-u)[1+\mu(\sqrt{1-z}/u)]}\right], \tag{51}$$

$$l_3^\infty(\mu) = \mu^2 n_f^2\left(\frac{1-\Omega_\nu}{1-z}\right)\left[1 - \left(\frac{a_2}{b_2}\right) \times \frac{2z}{w_+(1-u)[1+\mu(\sqrt{1-z}/u)]}\right]. \tag{52}$$

Equation (49) shows the importance of the substrate emittance $\epsilon_{\nu s}$. For small $K_{\nu d}$ the film emittance is dominated by $\epsilon_{\nu s}$. In order to have an efficient thin-film selective emitter the substrate spectral emittance outside the desired emittance band must be small. This is discussed further in the following section. For very thick films the substrate emittance makes no contribution to the film emittance, as Eq. (50) illustrates.

Figure 2 shows ϵ_ν vs $K_{\nu d}$ [Eq. (48)] at several values of the scattering albedo Ω_ν for a substrate emittance $\epsilon_{\nu s}=0.1$. Also, reflectivities at the interfaces are zero ($\rho_{\nu s}=\rho_{\nu 0}=0$) so that $n_0=n_f=n_s=1$ and $\mu_M=0$. Values for the constants used in the exponential integral approximations [Eq. (A2)] were taken from Ref. 18 ($a_1=b_1=2$) and Ref. 17 ($a_2=\frac{3}{4}$,

$b_2=\frac{1}{2}$). Also, shown in Fig. 2 is the linear approximation [Eq. (49)] for the case $\Omega_v=0$. Obviously the linear approximation applies only very close to $K_{vd}=0$. In the emitter efficiency calculations to follow the optical depths of interest are greater than 0.5; therefore, the linear approximations cannot be used. For the case $\Omega_v=1$ ($a_v=0$), when the film emits no radiation only the substrate contributes to ϵ_v.

III. EFFICIENCY OF THIN-FILM SELECTIVE EMITTER

Knowing ϵ_v allows the calculation of the efficiency of a thin-film selective emitter. The work of Nelson and Parent[14,15] shows that the emission spectra of the rare-earth oxides neodymia (Nd_2O_3), holmia (Ho_2O_3), erbia (Er_2O_3), and ytterbia (Yb_2O_3) are dominated by a single, narrow strong emission band. Therefore, to simplify the analysis, the emittance of the film is split into three regions of constant optical properties. For the region of photon energy ($E=h\nu$) below the emission band the emittance is ϵ_l, which will be a function of the optical depth K_l, scattering albedo Ω_l, substrate emissivity ϵ_{sl}, reflectivity of film-vacuum interface ρ_{0l}, and reflectivity of film-substrate interface ρ_{sl},

$$\epsilon_l=\epsilon_l(K_l,\Omega_l,\epsilon_{sl},\rho_{0l},\rho_{sl}). \tag{53a}$$

Similarly the emittance in the emission band is ϵ_g and the emittance for photon energies greater than the emission band is ϵ_u,

$$\epsilon_g=\epsilon_g(K_g,\Omega_g,\epsilon_{sg},\rho_{0g},\rho_{sg}), \tag{53b}$$

$$\epsilon_u=\epsilon_u(K_u,\Omega_u,\epsilon_{su},\rho_{0u},\rho_{su}). \tag{53c}$$

In Eq. (53) K_g is the optical depth for the emission band, K_u is the optical depth for photon energies greater than the emission band photon energy ($E>E_g=h\nu_g$). Similarly, Ω_g and Ω_u, ϵ_{sg} and ϵ_{su}, ρ_{0g} and ρ_{0u}, as well as ρ_{sg} and ρ_{su} are the scattering albedos, substrate emittances, film-vacuum reflectivity, and film-substrate reflectivity for the emission-band and above-emission-band regions, respectively.

Now define the emitter efficiency as follows:

$$\eta_E=\frac{\text{emitted power from emission band}}{\text{total emitted power}}. \tag{54}$$

Using the three emittances just discussed, the efficiency becomes

$$\eta_E=\frac{\epsilon_g\int_{E_g-\Delta E_g/2}^{E_g+\Delta E_g/2}e_{Eb}\,dE}{\epsilon_l\int_0^{E_g-\Delta E_g/2}e_{E_b}\,dE+\epsilon_g\int_{E_g-\Delta E_g/2}^{E_g+\Delta E_g/2}e_{Eb}\,dE+\epsilon_u\int_{E_g+\Delta E_g/2}^{\infty}e_{Eb}\,dE}, \tag{55a}$$

$$\eta_E=\left[1+\frac{\epsilon_l}{\epsilon_g}G\left(\frac{E_g}{kT_E},\frac{\Delta E_g}{E_g}\right)+\frac{\epsilon_u}{\epsilon_g}H\left(\frac{E_g}{kT_E},\frac{\Delta E_g}{E_g}\right)\right]^{-1}, \tag{55b}$$

where $e_{Eb}(E,T_E)$ is the blackbody emissive power [Eq. (6)] in terms of photon energy $E=h\nu$ and emitter temperature T_E. The photon energy at the center of the emission band is E_g and ΔE_g is the width of the emission band. Also, using Eq. (6) for e_{Eb} in Eq. (55) yields

$$G(s,t)=\left(\frac{\pi^4}{15}-\int_{s(1-t/2)}^{\infty}\frac{x^3}{e^x-1}\,dx\right)\Big/\left(\int_{s(1-t/2)}^{s(1+t/2)}\frac{x^3}{e^x-1}\,dx\right), \tag{56}$$

$$H(s,t)=\left(\int_{s(1+t/2)}^{\infty}\frac{x^3}{e^x-1}\,dx\right)\Big/\left(\int_{s(1-t/2)}^{s(1+t/2)}\frac{x^3}{e^x-1}\,dx\right). \tag{57}$$

As Eq. (55) indicates η_E is a function of E_g/kT_E, $\Delta E_g/E_g$, and the emittance ratios ϵ_l/ϵ_g and ϵ_u/ϵ_g. And as Eqs. (53a)–(53c) show, the emittance ratios are functions of the film and substrate optical properties. For given values of E_g/kT_{E_g} and $\Delta E_g/E_g$ there will be an optimum film thickness that will maximize η_E.

To simplify the presentation of results, define the optical properties below and above the emission band in terms of the emission-band properties. Therefore, for the extinction coefficients ($\alpha=a+\sigma$),

$$\alpha_l\equiv a_l+\sigma_l=f_l(a_g+\sigma_g) \quad \text{or} \quad K_l=f_lK_g, \tag{58a}$$

$$\alpha_u=a_u+\sigma_u=f_u(a_g+\sigma_g) \quad \text{or} \quad K_u=f_uK_g, \tag{58b}$$

and for the scattering albedo [$\Omega=\sigma/(a+\sigma)$],

$$\Omega_l=g_l\Omega_g, \tag{59a}$$

$$\Omega_u=g_u\Omega_g, \tag{59b}$$

and for the substrate emittance (ϵ_s),

$$\epsilon_{sl}=h_l\epsilon_{sg}, \tag{60a}$$

$$\epsilon_{su}=h_u\epsilon_{sg}. \tag{60b}$$

Now the emittance ratios ϵ_l/ϵ_g and ϵ_u/ϵ_g that appear in η_E are determined by the emission-band optical properties, the interface reflectivities, and the f, g, and h parameters. To obtain the maximum efficiency $\eta_{E_{\text{opt}}}$ for given values of E_g/kT_E and $\Delta E_g/E_g$ and the f, g, and h parameters, the optical depth K_g must be varied until Eq. (55) is a maxi-

mum. This optimization process was carried out on a personal computer using MATHEMATICA[19] software.

Consider the case where the substrate, film, and vacuum surroundings all have the same index of refraction ($n_s=n_f=n_0=1$). In this case $\mu_m=0$ and $\rho_{v0}=\rho_{vs}=0$. The optimum efficiency $\eta_{E_{opt}}$ as a function of E_g/kT_E for several values of the substrate emittance ϵ_{sg} are shown for this case in Fig. 3. Figure 3(a) is for no scattering ($\Omega=0$) and Fig. 3(b) is for equal scattering and an absorption coefficient (Ω of 0.5). It is assumed that $\Delta E_g/E_g=0.1$, which is typical for the rare-earth oxides considered by Nelson and Parent[14,15], $g_l=g_u=h_l=h_u=1$ and that $f_l=f_u=0.01$, since f, g, and h are the same for both above- and below-emission-band regions, $\epsilon_u=\epsilon_l$, and there is a single optimum optical depth independent of E_g/kT_E, $K_{g_{opt}}$, for maximum η_E. If f, g, and h are different above and below the emission band then there will be a different $K_{g_{opt}}$ that yields $\eta_{E_{opt}}$ for each value of E_g/kT_E. The optimum optical depth for each value of ϵ_{sg} is listed in Fig. 3. For Fig. 4 the same conditions were used as in Fig. 3 except that $f_u=f_l=0.1$. In other words, the extinction coefficient below and above the emission band is a factor of 10 higher in Fig. 4.

From the work of Nelson and Parent[14,15] with the rare-earth oxides already mentioned, it is expected that f_u and f_l should be in the range of 0.01–0.1. Thus, Figs. 3 and 4 should be representative of the range of emitter efficiencies that can be expected from a thin-film rare-earth oxide selective emitter. For $f_u=f_l=0.01$ maximum efficiencies up to 0.7 are expected and for $f_u=f_e=0.1$ maximum efficiencies of 0.35 are expected. There are several important conclusions to be made based on the results shown in Figs. 3 and 4. First of all, by comparing Fig. 3(a) with Fig. 3(b) and Fig. 4(a) with Fig. 4(b) it can be seen that, for $\Omega_u=\Omega_l=\Omega_g\leqslant 0.5$, scattering has a negligible effect on the magnitude of the optimum efficiency; however, to obtain $\eta_{E_{opt}}$ with scattering requires larger optical depths. With scattering the same at all photon energies, we expect scattering to have negligible effect on $\eta_{E_{opt}}$ since it is the emissive properties (absorption coefficient) that should determine η_E. Scattering will reduce the emission (Fig. 2) but it will not greatly alter the emittance ratios ϵ_u/ϵ_g and ϵ_l/ϵ_g that determine η_E [Eq. (55)]. Second, the importance of a low-emittance substrate in order to have high efficiency is evident from Figs. 3 and 4. The range of E_g/kT_E for attaining large η_E also decreases for smaller ϵ_{sg}. Also, the optimum optical depth increases as ϵ_{sg} increases. As f_u and f_l increase, the effect of the substrate emittance is reduced. Finally, the maximum efficiency in all cases occurs at $E_g/kT_E\approx 4$. This result was obtained by Chubb[16] using Eq. (55) for a selective emitter with assumed values for ϵ_u/ϵ_g and ϵ_l/ϵ_g in the range of 0.01–0.2. If $f_l>f_u$ the optimum value for E_g/kT_E is reduced (higher T_E required for given E_g). Table I shows the optimum temperature ($E_g/kT_E=4$) for four of the rare-earth oxides when $f_u=f_l$. For Yb_2O_3 and Er_2O_3, reaching the optimum temperature ($T_{E_{opt}}>3000$ K) means that Yb_2O_3 and Er_2O_3 will melt; however, for Ho_2O_3 and Nd_2O_3 the optimum temperature should be attainable.

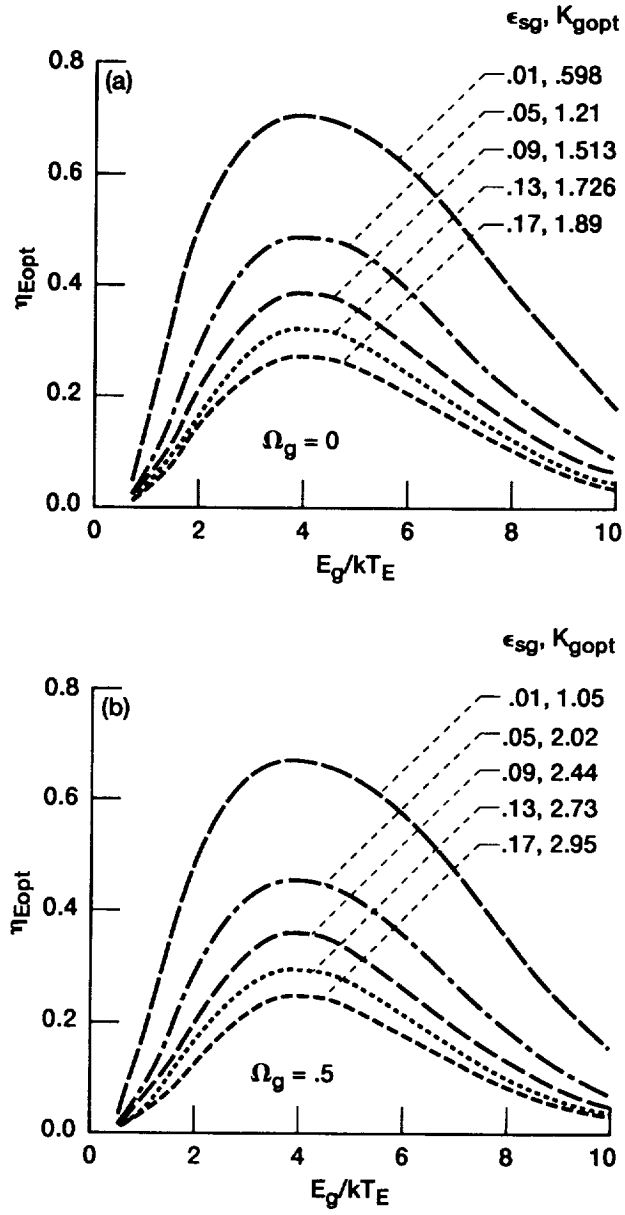

FIG. 3. Dependence of optimum emitter efficiency $\eta_{E_{opt}}$, on dimensionless emission-band energy, using the optimum optical depth $K_{g_{opt}}$, for both below-emission-band and above-emission-band optical depths equal to 0.01 (emission-band optical depth) ($f_l=f_u=0.01$). Also, substrate emittance is constant ($h_u=h_l=1$), no reflectance at interfaces ($\rho_{v0}=\rho_{vs}=0$), and $\Delta E_g/E_g=0.1$. (a) No scattering ($\Omega_l=\Omega_u=\Omega_g=0$); (b) equal scattering and absorption coefficients ($\Omega_l=\Omega_u=\Omega_g=0.5$).

Figure 5 shows the dependence of efficiency on optical depth for no scattering ($\Omega_l=\Omega_u=\Omega_g=0$). In Fig. 5(a) the efficiency is shown as a function of K_g for the same conditions as in Fig. 3(a) but with E_g/kT_E fixed at the value for optimum efficiency ($E_g/kT_E=4$). Figure 5(b) shows η_E vs K_g for the same conditions as Fig. 4(a), again with $E_g/kT_E=4$. When the emission-band extinction coefficient is much greater than the below-band and above-band extinction coefficients ($f_u=f_l=0.01$) then near-optimum efficiency is attained as long as $K_g\geqslant 1$. However, for $f_u=f_l=0.1$ optimum efficiency is achieved only when $K_g\leqslant 1$. The optimum optical depths for $f_u=f_l=0.1$ [Fig.

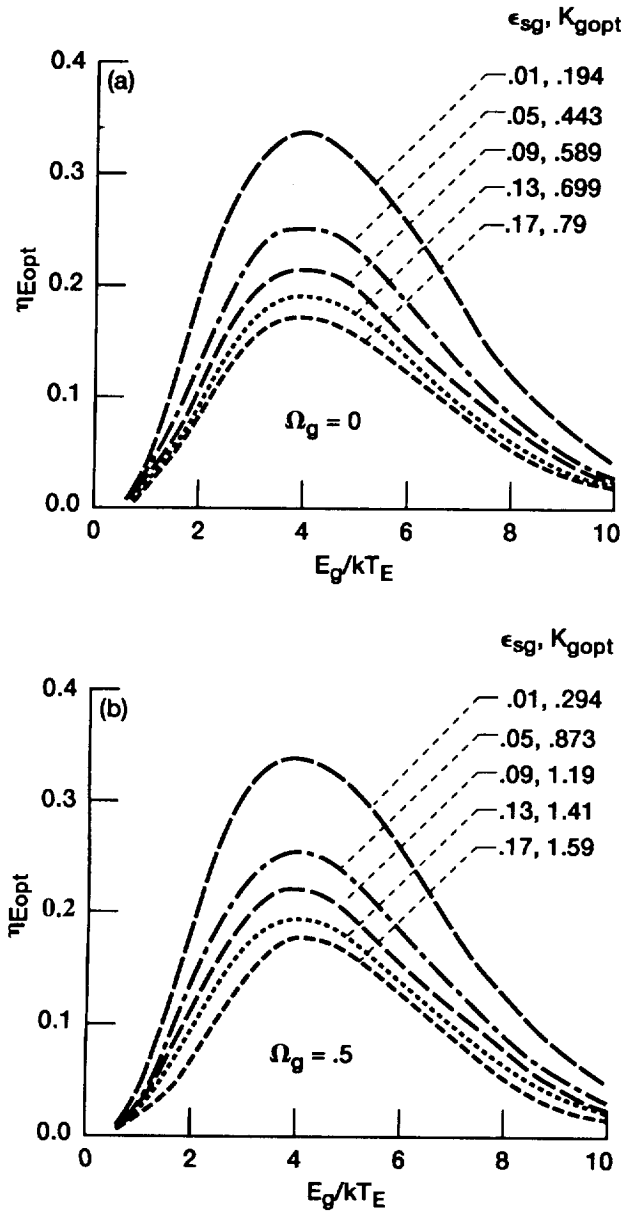

FIG. 4. Dependence of optimum emitter efficiency $\eta_{E_{opt}}$, on dimensionless emission-band energy E_g/kT_E, using the optimum optical depth $K_{g_{opt}}$ for both below-emission-band and above-emission-band optical depths equal to 0.1 (emission-band optical depth) ($f_l=f_u=0.1$). Also, the substrate emittance is constant ($h_l=h_u=1$), no reflectance at interfaces ($\rho_{v0}=\rho_{vs}=0$), and $\Delta E_g/kT_E=0.1$. (a) No scattering ($\Omega_l=\Omega_u=\Omega_g=0$); (b) equal scattering and absorption coefficients ($\Omega_l=\Omega_u=\Omega_g=0.5$).

5(b)] are more than a factor of 2 less than those for $f_u=f_l=0.01$ [Fig. 5(a)]. As stated earlier, the rare-earth oxides are expected to have f_u and f_l values between 0.01 and 0.1.

The dependence of efficiency on optical depth for the case of equal scattering and absorption coefficients ($\Omega_l=\Omega_u=\Omega_g=0.5$) is shown in Fig. 6. Comparing Figs. 5 and 6 shows that scattering has negligible effect on the magnitude of η_E. Scattering merely results in the maximum η_E occurring at larger K_g than for the nonscattering case. These results were also deduced from Figs. 3 and 4.

Now consider the importance of the interface reflectivities ρ_{v0} and ρ_{vs}. Equation (48) shows that the major contribution to ϵ_v of the vacuum-film interface reflectivity is the $(1-\rho_{v0})$ term. Therefore, if ρ_{v0} is a constant this term will cancel in the ratios ϵ_l/ϵ_g and ϵ_u/ϵ_g that appear in η_E [Eq. (55a)]. As a result, the ρ_{vs} term in Eq. (48) will have the major effect on η_E rather than ρ_{v0}.

To determine just how important ρ_{v0} and ρ_{vs} are in determining η_E we approximated the reflectivities in the following manner. For the vacuum-film interface the normal reflectivity for a specular reflective dielectric interface was used:[17]

$$\rho_{v0}=\left(\frac{n_f-1}{n_f+1}\right)^2. \tag{61}$$

Also, since $n_f>1$ the maximum incidence angle θ_M that allows radiation to escape the film is no longer $\pi/2$ but is given by Eq. (13). There are limited data available on n_f as a function of wavelength for rare-earth oxides. Marcinow and Truszkowska[20] found that n_f for Gd_2O_3, Eu_2O_3, Er_2O_3, and Yb_2O_3 is nearly constant for $0.5\leqslant\lambda\leqslant2.5$ μm. Also, they found that $1.85\leqslant n_f\leqslant1.95$ for these four rare-earth oxides in the $0.5\leqslant\lambda\leqslant2.5$ μm wavelength region. The index of refraction data of Refs. 21 and 22 are in agreement with these results. Therefore, for the calculations a constant value of $n_f=1.9$ was chosen. As a result, $\rho_{v0}=0.096$ and $\mu_M=0.85$. As already discussed, the substrate must be a low-emittance ($\epsilon_s\leqslant0.05$) material. In a later discussion of substrate materials rhodium and copper are recommended as substrate materials. Since both copper and rhodium are opaque, $\rho_{vs}+\epsilon_{vs}=1$; therefore, $\rho_{vs}=1-\epsilon_{vs}$ was used in the calculations.

In Fig. 7 the effect of ρ_{v0} and ρ_{vs} on the optimum efficiency is presented for the same conditions as Fig. 3. Figure 7(a) is for no scattering and Fig. 7(b) is for equal scattering and absorption coefficients. Comparing Figs. 3 and 7 shows that there is about a 10% increase in $\eta_{E_{opt}}$ for $\epsilon_{sg}=0.01$, but at $\epsilon_{sg}=0.17$, $\eta_{E_{opt}}$ has increased by nearly a factor of 2 for $n_f=1.9$. Also note that the optimum optical depth is approximately a factor of 3 smaller. As discussed earlier this change results from ρ_{vs} rather than ρ_{v0} for a constant n_f. If n_f were strongly dependent on wavelength then the $(1-\rho_v)$ term in the emittance [Eq. (48)] would also depend on wavelength. Thus, the emittance ratios ϵ_l/ϵ_g and ϵ_u/ϵ_g that appear in η_E [Eq. (55a)] would also depend on wavelength. Therefore, in that case η_E could be significantly effected by ρ_{v0}.

IV. EMISSIVE POWER OF THIN-FILM SELECTIVE EMITTER

Other than efficiency, the power emitted in the emission band is the most important performance parameter for a thin-film selective emitter. This emitted power/area P_E is given by the numerator of Eq. (55). Now define the dimensionless power density as follows:

$$p_E\equiv\frac{P_E}{\sigma_{SB}T_E^4}=\frac{\epsilon_g\int_{E_g-\Delta E_g/2}^{E_g+\Delta E_g/2}e_{Eb}\,dE}{\int_0^\infty e_{Eb}\,dE}, \tag{62}$$

TABLE I. Emission-band data for rare-earth oxides.

Emitter material	Emission-band transition	Photon energy at center of emission band E_g (eV)	Photon wavelength at center of emission band (μm)	Dimensionless bandwidth $\Delta E_g/E_g$	Emitter temperature for maximum efficiency, $T_{E/\text{opt}}=\frac{1}{4}eE_g/k$ (K)
Ytterbia Yb_2O_3	$^2F_{5/2}$ to $^2F_{7/2}$	1.29	0.955	0.18	3740
Erbia Er_2O_3	$^4I_{13/2}$ to $^4I_{15/2}$	0.827	1.5	0.05	2400
Holmia Ho_2O_3	$^5I_7$ to $^5I_8$	0.62	2.0	0.10	1800
Neodymia Nd_2O_3	$^4I_{13/2}$ to $^4I_{9/2}$	0.52	2.4	0.15	1500

where σ_{SB} is the Stefan–Boltzmann constant ($\sigma_{SB}=5.67\times10^{-12}$ W/cm^2 K^4) and T_E is the emitter temperature. Using Eq. (6) for the blackbody emissive power e_{Eb} gives the following:

$$p_E=\frac{15}{\pi^4}\epsilon_g\int_{s(1-t/2)}^{s(1+t/2)}\frac{x^3}{e^x-1}\,dx, \tag{63}$$

where

$$s=\frac{E_g}{kT_E},\quad t=\frac{\Delta E_g}{E_g}. \tag{64}$$

The power density p_E behaves differently, as a function of optical depth, than the efficiency. As Figs. 5 and 6 show, there is an optimum optical depth for maximum efficiency. However, as Eq. (63) shows, p_E depends on optical depth only through ϵ_g. And as Fig. 2 shows ϵ_g is a monotonically increasing function of optical depth. As a result, p_E will also be a monotonically increasing function of optical depth. Also, the substrate emittance ϵ_{sg} will affect p_E only for small optical depths. Most important, however, is the effect of scattering on p_E. As discussed earlier, scattering has a negligible effect on the optimum efficiency; however, scattering reduces p_E since ϵ_g decreases with increasing Ω_g (Fig. 2). These points are illustrated in Fig. 8 where p_E is shown as a function of optical depth. Figure 8(a) is for the nonscattering case ($\Omega_g=0$) and Fig. 8(b) is for equal scattering and absorption coefficients ($\Omega_g=0.5$). Notice that p_E increases more rapidly for the nonscattering case. Near maximum p_E is attained at $K_g\geqslant1$; however, with scattering, $K_g\geqslant2$ for maximum p_E.

Figure 9 shows p_E as a function of E_g/kT_E for the same conditions as Fig. 8 with $K_g=1$ for the nonscattering case [Fig. 9(a)] and $K_g=2$ for $\Omega_g=0.5$ [Fig. 9(b)]. With these values of K_g the power densities will be close to their maximum values. Similar to η_E, p_E has its maximum value at $E_g/kT_E\approx4$; however, the location of maximum η_E and p_E will shift if f, g, and h are different below and above the emission band. This is illustrated in Fig. 10 where $\eta_{E_{\text{opt}}}$ and p_E are shown as functions of E_g/kT_E for $f_u=0.01$, $f_l=0.1$, $g_u=g_l=h_u=h_l=1$, $\Delta E_g/E_g=0.1$ with no scattering ($\Omega_g=0$) or reflectance at the interface and for two values of substance emittance ($\epsilon_{sg}=0.01$, 0.05). As stated earlier, when $f_l\neq f_u$ the optimum optical depth is a function of E_g/kT_E. Therefore, each point on the curves in Fig. 10 corresponds to a different optical depth. The power density p_E was calculated using the optimum optical depth. As can be seen, if $f_l>f_u$ the maximum efficiency and power density are shifted to a lower value of E_g/kT_E than is the case where $f_u=f_l$ (Figs. 3 and 4); however, the dependence of maximum p_E on E_g/kT_E is much less than the maximum efficiency dependence. Also note that p_E is significantly effected by the substrate emittance compared to Fig. 9 where K_g is a constant.

V. POSSIBLE SUBSTRATES FOR RARE-EARTH OXIDE THIN-FILM SELECTIVE EMITTERS

From the analytical results just discussed we know that a thin-film selective emitter must have a low-emittance substrate in order to have high efficiency; also, the substrate must have a high melting temperature. These two requirements greatly limit the choice for a substrate material. Copper, silver, and gold all have low emittance[23] ($\epsilon_s<0.1$), however, their melting points are also low. Copper with a melting point of 1356 K may be suitable for use with Nd_2O_3. For the high temperatures required by Er_2O_3, Ho_2O_3, and Yb_2O_3 two possible substrates are sapphire with a melting point of 2326 K and rhodium (Rh) with a melting point of 2233 K. Sapphire has low emittance ($\epsilon_{vs}<0.1$) for wavelengths $\lambda<4.0$ μm, however, for $5\leqslant\lambda\leqslant15$ μm the emittance is large.[23,24] Therefore, sapphire is most suitable for the highest temperatures ($T\geqslant2000$ K) where most of the radiation is at $\lambda<4$ μm. Rhodium has total emittance $\epsilon_s<0.1$ up to the highest temperature (1500 K) for which data are available.[23] As a result rhodium should be a suitable substrate for all the rare-earth oxides.

VI. CONCLUSION

Using a radiation transfer analysis that includes isotropic scattering an expression for the spectral emittance of a thin film was developed. Interference effects were neglected. Splitting the spectral optical properties of the rare-earth oxides into three regions (below emission band, emis-

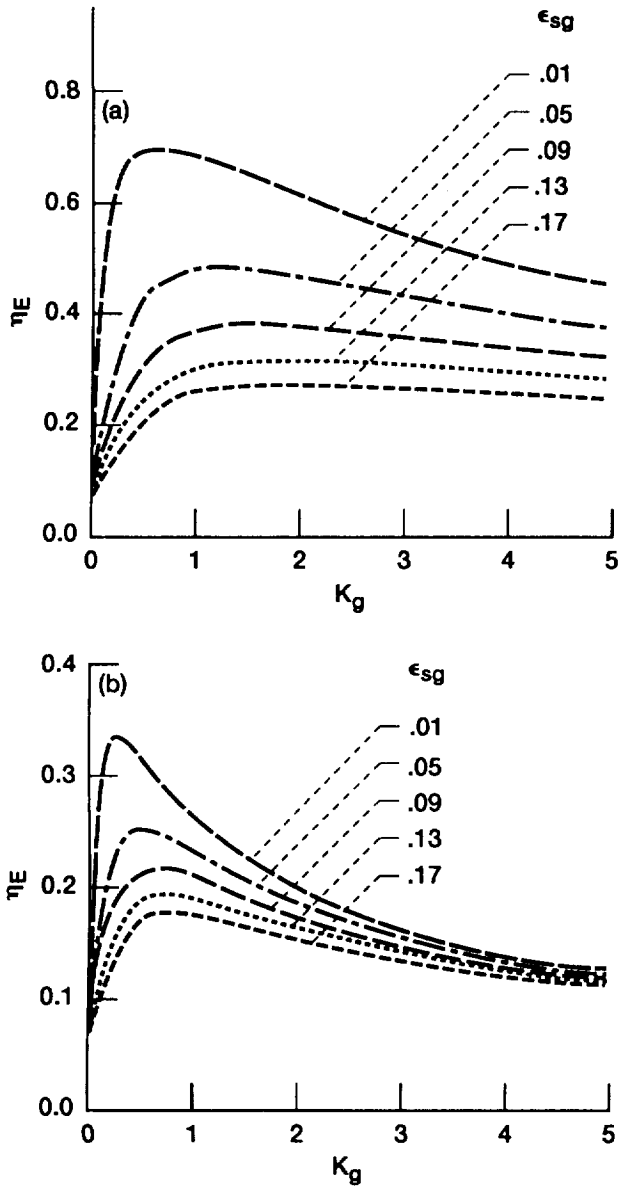

FIG. 5. Dependence of emitter efficiency η_E on emission-band optical depth K_g for no scattering ($\Omega_g=\Omega_u=\Omega_l=0$) and constant substrate emittance ($h_l=h_u=1$). Also, $E_g/kT_E=4$, $\Delta E_g/E_g=0.1$, and no reflectance at interfaces ($\rho_{v0}=\rho_{vs}=0$). (a) Both below- and above-emission-band optical depths equal to 0.01 (emission-band optical depth) ($f_u=f_l=0.01$); (b) both below- and above-emission-band optical depths equal to 0.1 (emission-band optical depth) ($f_l=f_u=0.1$).

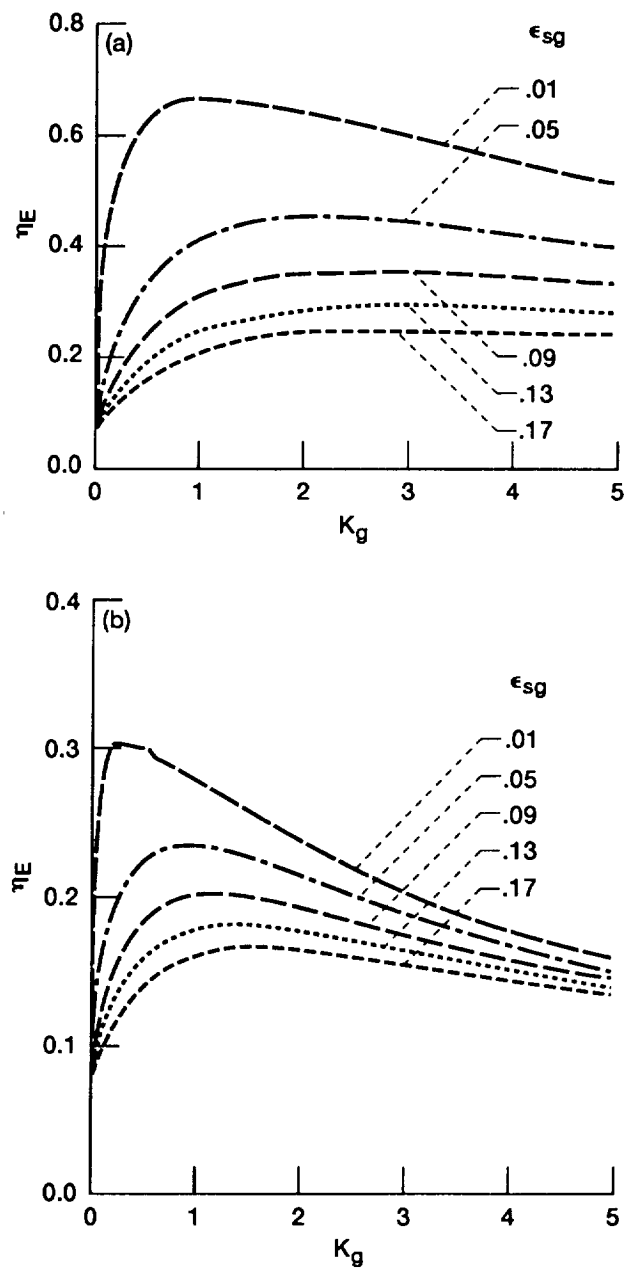

FIG. 6. Dependence of emitter efficiency η_E on emission-band optical depth K_g for equal scattering and absorption coefficients ($\Omega_g=\Omega_u=\Omega_l=0.5$) and constant substrate emittance ($h_u=h_l=1$). Also, $\Delta E_g/E_g=0.1$ and no reflectance at interfaces ($\rho_{v0}=\rho_{vs}=0$). (a) Both below- and above-emission-band optical depths equal to 0.01 (emission-band optical depth) ($f_u=f_l=0.01$); (b) both below- and above-emission-band optical depths equal to 0.1 (emission-band optical depth) ($f_l=f_u=0.1$).

sion band, and above emission band) and using the spectral emittance expression, the emitter efficiency η_E was calculated. Calculated optimum efficiencies range from $\eta_E\approx 0.35$ to $\eta_E\approx 0.7$.

Two important results of the analysis are the following. First, in order to achieve high efficiency the film substrate must have very low emittance ($\epsilon_s\leqslant 0.05$). Second, there is an optimum optical depth to obtain maximum η_E. For the scattering coefficient σ_v less than the or equal to the absorption coefficient a_v, scattering has a negligible effect on the optimum efficiency. However, the optical depth required to obtain maximum efficiency with scattering is greater than the optical depth required to obtain maximum efficiency without scattering. Also, scattering reduces the emissive power density. Finally, the maximum efficiency occurs when $E_g/kT_E\approx 4$, where E_g is the photon energy at the center of the emission band and T_E is the emitter temperature.

The low-emittance and high-temperature requirements on the substrate severely limit the choice of substrate material. Copper may be suitable for use with Nd_2O_3. For the

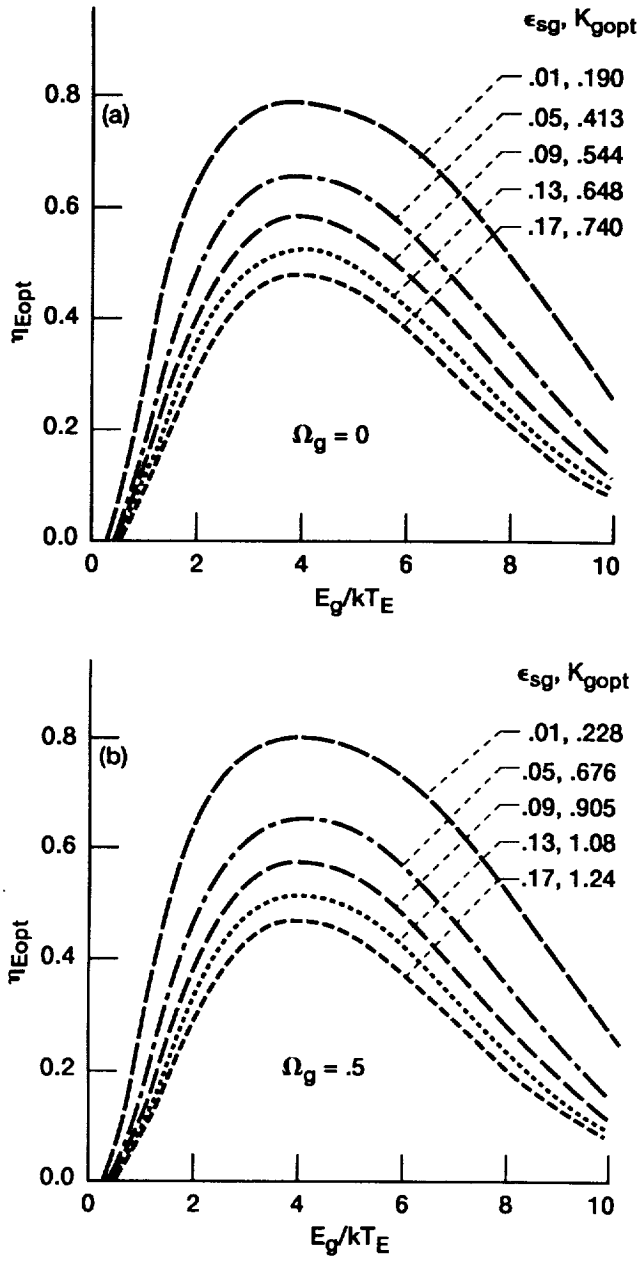

FIG. 7. Effect of finite reflectance at vacuum-film interface ρ_{v0} and film-substrate interface ρ_{vs} on optimum efficiency $\eta_{E_{opt}}$. ρ_{v0} given by the reflectance for normal incidence [Eq. (61)], $n_f=1.9$, $\rho_{v0}=0.096$, and $\rho_{vs}=1-\epsilon_{sg}$. Also, $f_l=f_u=0.01$, $g_l=g_u=1$, $h_l=h_u=1$, and $\Delta E_g/E_g=0.1$. (a) No scattering ($\Omega_u=\Omega_g=\Omega_l=0$); (b) equal scattering and absorption coefficients ($\Omega_u=\Omega_g=\Omega_l=0.5$).

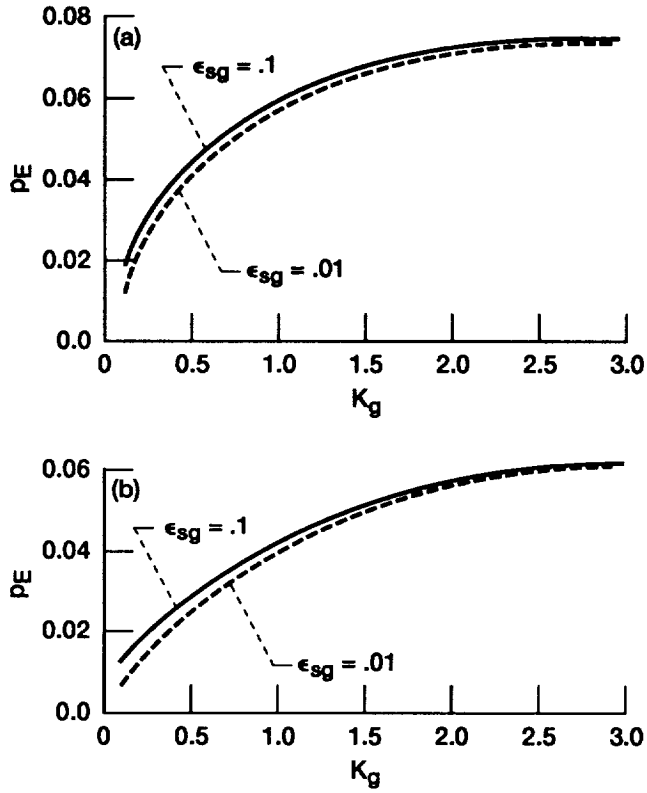

FIG. 8. Dependence of dimensionless emitter power density, $p_E=P_E/\sigma_{SB}T_E^4$, on emission-band optical depth K_g for substrate emittance $\epsilon_{sg}=0.01$ and 0.05. Also, $E_g/kT_E=4$, $\Delta E_g/E_g=0.1$, and no reflectance at interfaces ($\rho_{v0}=\rho_{vs}=0$). (a) No scattering case ($\Omega_g=0$) and $K_g=1.0$; (b) equal scattering and absorption coefficients ($\Omega_g=0.5$) and $K_g=2.0$.

other rare-earth oxides, sapphire and rhodium are possible substrate choices.

APPENDIX: SOURCE FUNCTION SOLUTION

Equation (3) must be solved for the source function $S_v(K_v)$ that appears in the radiative transfer Eqs. (1) and (2). Since the boundaries are assumed to behave diffusely, $i_v^+(0,\mu)$ and $i_v^-(K_{ve},-\mu)$ are independent of μ and Eq. (3) becomes the following:

$$S_v(K_v)=n_f^2(1-\Omega_v)\frac{e_{vb}}{\pi}+\frac{\Omega_v}{2}\left(E_2(K_v)\frac{q^+(0)}{\pi}+E_2(K_{vd}-K_v)\frac{q^-(0)}{\pi}+\int_0^{K_{vd}}S_v(K_v^*)\times E_1(|K_v^*-K_v|)dK_v^*\right). \quad \text{(A1)}$$

In order to reduce this integral equation for S_v to a differential equation, the exponential integrals are approximated as follows:

$$E_n(x)=a_n\exp(-b_nx). \quad \text{(A2)}$$

For $E_1(x)$ the values $a_1=b_1=2$ were used in calculations, which is the same approximation used in Ref. 18. It should be noted that $E_1(0)\to\infty$; however, the approximation given by Eq. (A2) for $E_1(x)$ yields $E_1(0)=a_1$. For $E_2(x)$ the approximations $a_2=3/4$, $b_2=3/2$ were used.[17]

To convert Eq. (A1) to a differential equation, use the approximations given by Eq. (A2) for E_1 and E_2 and then take the second derivative with respect to K_v. This yields

$$\frac{d^2S_v}{dK_v^2}-\alpha_1S_v=-\alpha_2+\alpha_3\exp(-b_2K_v)+\alpha_4\exp(b_2K_v), \quad \text{(A3)}$$

where

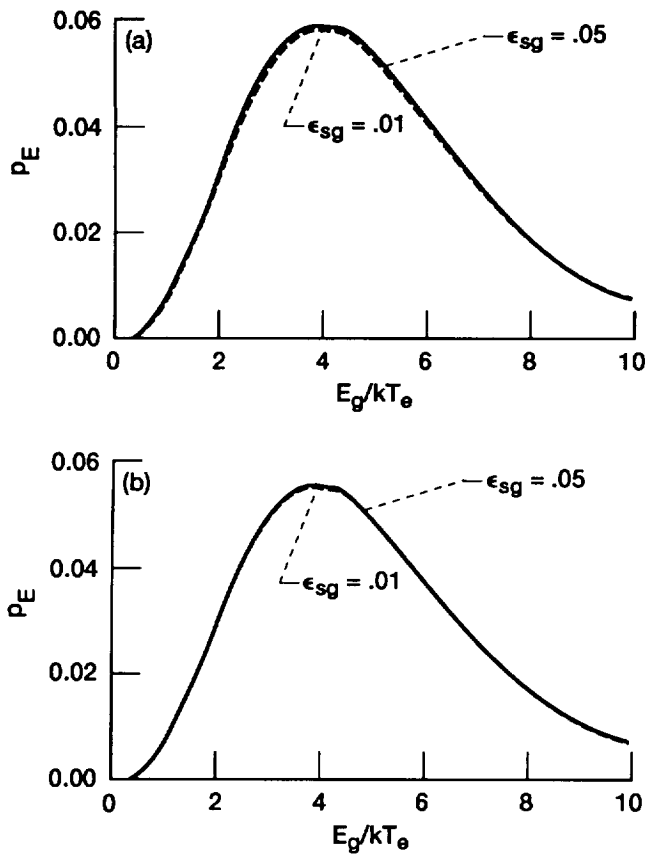

FIG. 9. Dependence of dimensionless emitter power density, $p_E=P_E/\sigma_{SB}T_E^4$, on dimensionless emission-band energy E_g/kT_E for substrate emittance $\epsilon_{sg}=0.01$ and 0.05. Also, $\Delta E_g/E_g=0.1$ and no reflectance at interfaces ($\rho_{v0}=\rho_{vs}=0$). (a) No scattering ($\Omega_g=0$) and $K_g=1.0$; (b) equal scattering and absorption coefficients ($\Omega_g=0.5$) and $K_g=2.0$.

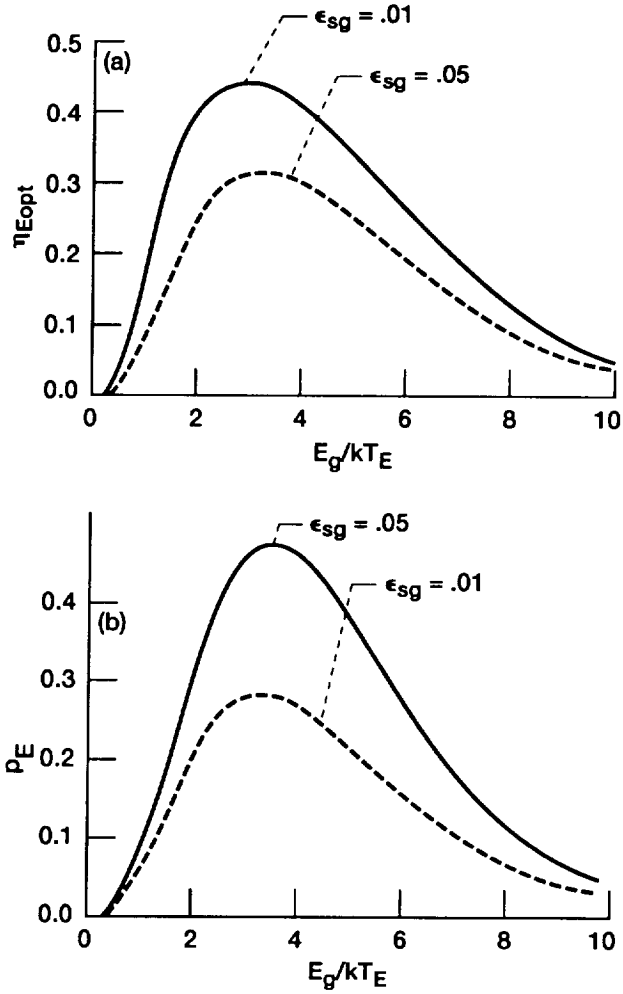

FIG. 10. Effect of unequal below-emission-band optical depth f_l and above-emission-band optical depth f_u ($f_l=0.1, f_u=0.01$) on optimum efficiency $\eta_{E_{opt}}$ and dimensionless power density p_E. Also, no scattering ($\Omega_u=\Omega_l=\Omega_g=0$), constant substrate emittance ($h_u=h_l=1$), $\Delta E_g/E_g=0.1$, and no reflectance at interfaces ($\rho_{v0}=\rho_{vs}=0$).

$$\alpha_1=b_1^2\left(1-\frac{a_1\Omega_v}{b_1}\right), \tag{A4}$$

$$\alpha_2=n_f^2(1-\Omega_v)b_1^2\frac{e_{vb}}{\pi}, \tag{A5}$$

$$\alpha_3=-\frac{a_2\Omega_v}{2}(b_1^2-b_2^2)\frac{q^+(0)}{\pi}, \tag{A6}$$

$$\alpha_4=-\frac{a_2\Omega_v}{2}(b_1^2-b_2^2)\frac{q^-(K_{vd})}{\pi}\exp(-b_2K_{vd}). \tag{A7}$$

The solution to this linear second-order differential equation is

$$S_v(K_v)=C_1\exp(\sqrt{\alpha_1}K_v)+C_2\exp(-\sqrt{\alpha_1}K_v)+C_3\exp(-b_2K_v)+C_4\exp(b_2K_v)+C_5, \tag{A8}$$

where the constants (C_1, C_2, C_3, C_4, and C_5) must satisfy Eqs. (A1) and (A3). If Eq. (A8) is substituted in Eq. (A3) then results for C_3, C_4, and C_5 are obtained. Using those results for C_3, C_4, and C_5 and then substituting Eq. (A8) in Eq. (A1) will yield (after a great deal of algebra) results for C_1 and C_2:

$$C_1=-\frac{A_4}{\pi}[A_1q_v^+(0)-A_2q_v^-(K_{vd})+A_3n_f^2e_{vb}]e^{-r}, \tag{A9}$$

$$C_2=\frac{A_4}{\pi}[A_2q_v^+(0)-A_1q_v^-(K_{vd})+A_3n_f^2e_{vb}], \tag{A10}$$

$$C_3=\frac{\alpha_3}{b_2^2-\alpha_1}=\frac{\gamma}{\pi}q_v^+(0), \tag{A11}$$

$$C_4=\frac{\alpha_4}{b_2^2-\alpha_1}=\frac{\gamma}{\pi}e^{-y}q_v^-(K_{vd}), \tag{A12}$$

$$C_5=\frac{1}{\pi}\frac{1-\Omega_v}{1-z}n_f^2e_{vb}. \tag{A13}$$

The quantities A_1, A_2, A_3, A_4, r, y, z, and γ are given by Eqs. (32)–(41). For no scattering, $\Omega_v=z=\gamma=A_4=0$ and all the C's vanish except C_5. Thus, as expected, only the blackbody emissive power e_{vb} contributes to the source term.

[1] D. C. White, B. D. Wedlock, and J. Blair, in Proceedings of the 15th Annual Power Sources Conference, 1961.
[2] B. D. Wedlock, Proc. IEEE **51**, 694 (1963).
[3] R. M. Swanson, Proc. IEEE **67**, 446 (1979).
[4] R. L. Bell, Sol. Energy **23**, 203 (1979).
[5] P. Würfel and W. Ruppel, IEEE Trans. Electron Devices **ED-27**, 745 (1980).
[6] W. Spirkl and H. Ries, J. Appl. Phys. **57**, 4409 (1985).
[7] H. Höfler, P. Würfel, and W. Ruppel, Sol. Cells **10**, 257 (1983).
[8] M. D. Morgan, W. E. Horne, and P. R. Brothers, AIP Conf. Proc. **271**, 313 (1993).
[9] D. L. Chubb, D. J. Flood, and R. A. Lowe, in Proceedings of NTSE-92 Nuclear Technologies for Space Exploration, 1992, p. 281.
[10] L. Block, P. Daugioda, and M. Goldstein, IEEE Trans. Industry Appl. **IA-28**, 251 (1992).
[11] D. C. White and R. J. Schwartz, in *Combustion and Propulsion, 6th AGARD Colloquium on Energy Sources and Energy Combustion*, edited by H. M. Degraff, J. Fabri, R. Haglund, T. F. Nagey, and R. E. Rumbauch, Jr. (Gordon Breach, New York, 1967), pp. 897–922.
[12] G. E. Guazzoni, Appl. Spectra **26**, 60 (1972).
[13] G. H. Dieke, *Spectra and Energy Levels of Rare Earth Ions in Crystals* (Interscience, New York, 1968).
[14] R. E. Nelson, in *Proceedings of the 32nd International Power Sources Symposium* (Electrochemical Society, Pennington, NJ, 1986), pp. 95–101.
[15] C. R. Parent and R. E. Nelson, in *Proceedings of the Twenty-First Intersociety Energy Conversion Engineering Conference* (American Chemical Society, Washington, DC, 1986), Vol. 2, pp. 1314–1317.
[16] D. L. Chubb, in *Proceedings of the 21st Photovoltaic Specialists Conference* (IEEE, New York, 1990), pp. 1326–1342; also NASA TM-103 290, 1990.
[17] R. Siegel and J. R. Howell, *Thermal Radiation Heat Transfer*, 2nd ed. (Hemisphere, Washington, DC, 1981), Chap. 14, 19-6.2, p. 96.
[18] B. F. Armalz, T. T. Lam, and A. L. Crosbie, AIAA J. **11**, 1498 (1973).
[19] S. Wolfram, *Mathematica: A System for Doing Mathematics by Computer*, 2nd ed. (Addison-Wesley, Redwood City, CA, 1991).
[20] T. Marcinow and K. Truszkowska, Appl. Opt. **20**, 1755 (1981).
[21] A. V. Dement'ev, G. D. Pridatko, and B. P. Kryzhanovskii, Sov. J. Opt. Technol. **44**, 35 (1977).
[22] A. F. Andreeva and I. Ya. Gil'man, Zh. Prikl. Spektros. **28**, 895 (1978).
[23] Y. S. Touloukian and D. P. DeWitt, *Thermophysical Properties of Matter* (Plenum, New York, 1970), Vol. 7.
[24] J. R. Markham, P. R. Solomon, and P. E. Best, Rev. Sci. Instrum. **61**, 3700 (1990).